OLYMPUS

Your Vision, Our Future

Microscope Objectives

Specialty Objectives

Advance Your Research with Specialty Objectives

Olympus' Leading–Edge Objectives Enable Innovative Research

Olympus has a history of developing high–quality objectives for advanced applications that contribute to the life science industry. We work with our customers to develop new, innovative products that meet both the evolving and specific needs of researchers in the field.

Our commitment to innovative optical technologies is exemplified by our multi photon excitation dedicated objectives, which we developed in response to the growing need for deep tissue observation in life science research. When our customers needed an optical system designed for live cell and *in vivo* 3D imaging, we developed silicone immersion objectives that enable researchers to capture brght, high–resolution images deeper within samples.

For more than 90 years, Olympus has manufactured advanced microscope equipment and high–quality objectives, and we are proud of our record of innovation and collaboration. We continue to work with researchers to develop new technologies that meet the changing needs of life science research.

Index

Multi Photon Excitation (MPE) Dedicated Objectives 3–4

Silicone Immersion Objectives 5–6

TIRF (Total Internal Reflected Fluorescence) Objectives 7–8

Super–Corrected 60X Objective 9

Time Saving Objective for Plastic Bottom Plates and Dishes 10

The Importance of Choosing the Right Objective and Correction Collar Adjustment

Choosing the right objective

One of the most important factors in acquiring higher resolution images is selecting the right objective. Matching the refractive index of the sample and immersion medium the objective can compensate for spherical aberration resulting in deeper, brighter, and higher resolution imaging. Most Olympus specialty objectives have high numerical apertures (NAs) and correction collars that enable users to compensate for spherical aberration, enhancing image resolution and contrast.

The importance of a correction collar

Spherical aberration is influenced by refractive index mismatches in the optical path, e.g. varying thickness of coverslips, observation depth of the sample, composition of cells or tissues, and changes in temperature. High NA objectives are particularly susceptible to these effects. Adjusting the correction collar of your objective is essential to compensate for spherical aberration to improve image quality (higher resolution, brighter, and higher contrast).

Comparison image of *in vivo* mouse brain sensory cortex before adjustment (left) and after adjustment (right).

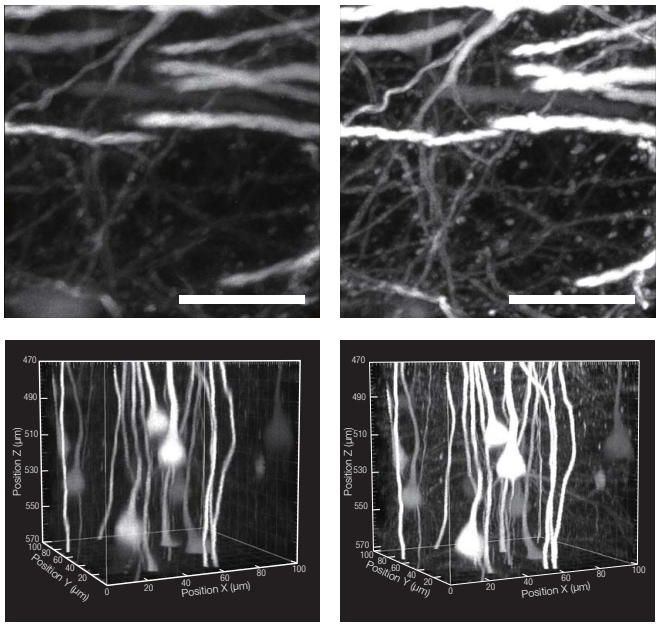

Upper figures: XZ image at 500 µm depth; scale bar represents 20 µm.
Lower figures: XYZ image at 470–570 µm depth.

Sample: Th1–YFP–H mouse

Comparison of oil and silicone immersion 60X objectives in a glycerol–mounted Drosophila brain.

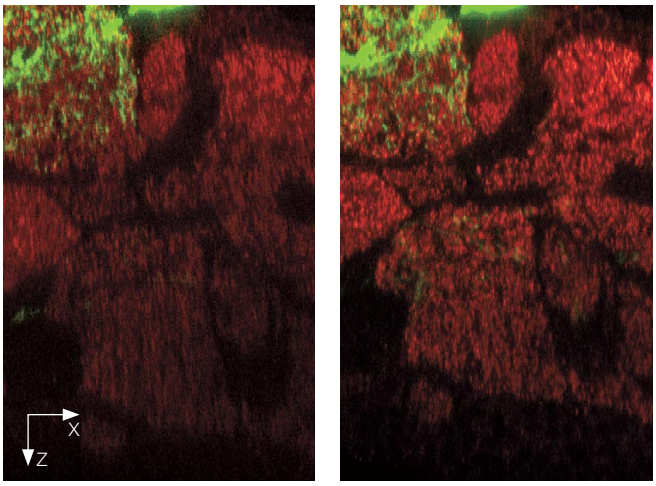

Oil immersion

Silicone immersion

mCD8 (GFP, Green)/a–Bruchpilot (Immunostaining, Red)

Image data courtesy of
Yasuhito Imanishi Ph.D., Hiromu Tanimoto Ph.D.
Tohoku University Graduate School of Life Sciences

Multi Photon Excitation Dedicated Objectives

Specially designed to achieve optimum performance with multi photon excitation imaging (MPE), these MPE dedicated objectives enable high–precision imaging of biological specimens to a depth of up to 8 mm for *in vivo* imaging and transparent sample imaging.

Selection guide of MPE dedicated objectives

	W.D. (mm)	MAG.	FN*	NA	Immersion (Refractive Index)	Sample	Purpose
XLPLN10XSVMP	8	10X	18	0.60	Water to oil (ne: 1.33 to 1.52)	*in vivo* and cleared sample	Wide FOV observation
XLSLPLN25XGMP	8	25X	18	1.00	Silicone oil to oil (ne: 1.41 to 1.52)	Cleared sample	High–resolution observation
XLSLPLN25XSVMP2	8	25X	18	0.95	Water to silicone oil (ne: 1.33 to 1.41)	*in vivo* and cleared sample	
XLPLN25XSVMP2	4	25X	18	1.00	Water to silicone oil (ne: 1.33 to 1.41)	*in vivo* and cleared sample	
XLPLN25XWMP2	2	25X	18	1.05	Water	*in vivo*	

*Maximum field number observable through eyepiece.

Deep *in vivo* Imaging: XLPLN25XWMP2

Deep *in vivo* multi photon brain imaging and optogenetics at high resolution require optimized objectives that not only have high transmission of IR light, but high NA and the ability to correct for the depth and scattering of tissue. The XLPLN25XWMP2 delivers ultra–broad IR transmission with the new 1600 coating, enabling optogenetic stimulation with visible light down to 400 nm and IR imaging or stimulation beyond 1600 nm. The correction collar reduced the excitation volume, enabling stimulation of single cells or dendritic spines. Combined with the powerful and precise scanning capabilities of the FVMPE–RS, the XLPLN25XWMP2 is the right tool for high–precision multi photon imaging.

in vivo Two Photon Imaging of Crossed Corticostriatal and Corticospinal Neurons in L5a During Learning

- Calcium imaging of deep a brain neuron circuit enables researchers to observe bright, quick responses of single neuron activity.

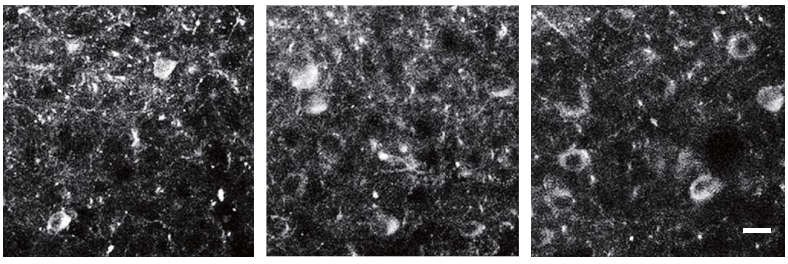

450 µm depth from brain surface 500 µm depth from brain surface 550 µm depth from brain surface

in vivo two photon imaging of crossed corticostriatal neurons transduced with rAAV2/9–Syn–GCaMP3 in the left forelimb M1 during learning of a motor task. 450, 500, and 550 µm depth from brain surface. Scale bar 20 µm.

Image data courtesy of Yoshito Masamizu Ph.D., Yasuhiro R Tanaka Ph.D., Masanori Matsuzaki Ph.D., Division of Brain Circuits, National Institute for Basic Biology
Reference: *Nat Neurosci.* 2014 Jul; 17 (7): 987–94. doi: 10.1038/nn.3739. Epub 2014 Jun 1.

in vivo Nephron Imaging at Kidney Surface

- High–resolution *in vivo* time–lapse imaging with NA 1.05.

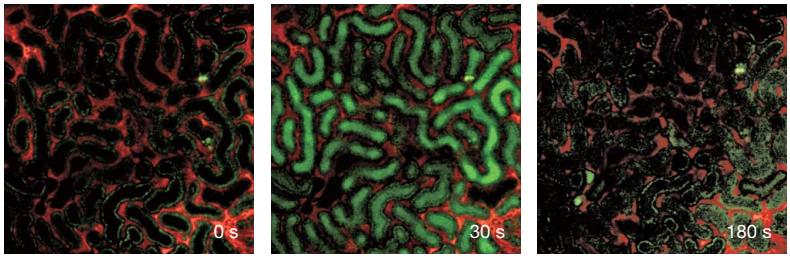

Time–lapse imaging of fluorescence dye (Lucifer Yellow, Green) injected into a vein that freely passes through the glomerulus. Red is rhodamine B labeled 70 kD dextran to observe the flow of blood plasma. The shadows in the blood plasma are blood cells. The green signal at 0 time is auto fluorescence of the proximal tubular cell.

Image data courtesy of Daisuke Nakano Ph.D., Department of Pharmacology, Faculty of Medicine, Kagawa University
Reference: *J Am Soc Nephrol.* 2015 Apr 8. pii: ASN.2014060577. [Epub ahead of print]

Deep Mouse Brain Imaging

- High NA and 2 mm working distance (W.D.) with optimized correction collar adjustments facilitate deep mouse brain imaging.

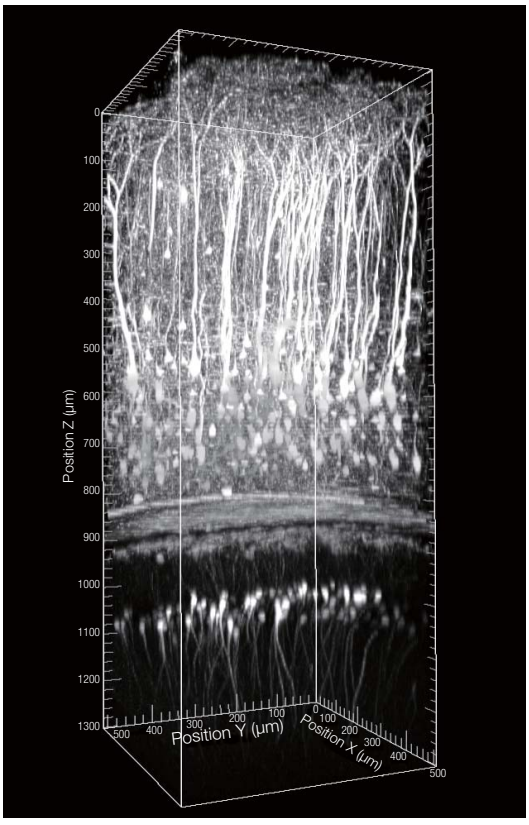

Z–stack image of *in vivo* mouse under anesthesia from the brain surface to the radiate layer of the hippocampus (CA1).

Sample: Thy1–YFP H line 8 week old male
Excitation wavelength: 960 nm
Image data courtesy of Katsuya Ozawa and Hajime Hirase, Neuron–Glia Circuitry, RIKEN Brain Science Institute, Japan

Deep Observation of Fixed Transparent Specimens with Multi Photon Objectives Down to a Depth of 8 mm

The Olympus MPE dedicated objectives help facilitate breakthrough research on brain function and other vital organs. Until recently, brain science researchers using light microscopes had to slice thin sections of tissue. With these new objectives and new tissue clearing technology, researchers can see as deep as 8 mm without slicing. The XLPLN25XSVMP2 and XLSLPLN25XSVMP2 were specifically designed and engineered for use with the revolutionary clearing reagent "Sca/e" developed by Dr. Atsushi Miyawaki and his team at the RIKEN Brain Science Institute in Japan.* Since then, there has been a proliferation of new clearing reagents including SeeDB, CLARITY, Sca/eS, and many others. The XLSLPLN25XGMP and XLPLN10XSVMP support these new reagents, enabling researchers to observe down to unprecedented depths. Using the objectives and clearing reagent together, tissue is made nearly transparent; scientists can now see the interconnections in brain and other tissues as never before.

*Published online in *Nature Neuroscience*: Hama et al. Aug 30, 2011

Whole Mouse Brain Imaging (XLPLN10XSVMP)

- Wide field of view with 10X magnification, single cell resolution with NA 1.0, observations down to 8 mm.
- Objectives match a wide range of clearing reagent refractive indices (ne: 1.33 to 1.52).

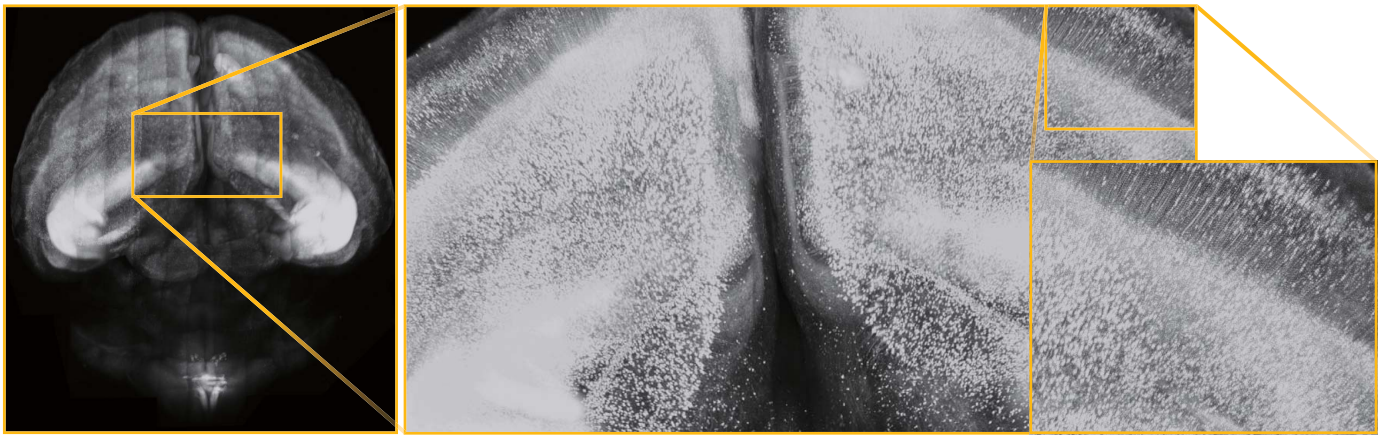

20 week old YFP–H mouse brain treated with Sca/eS

Single cell resolution

Image data courtesy of Hiroshi Hama, Atsushi Miyawaki, RIKEN Brain Science Institute Laboratory for Cell Function Dynamics

High–Resolution Deep Brain Imaging of Sca/eS Treated Mouse Brain (XLSLPLN25XGMP)

- High–resolution deep imaging with NA 1.0 and 8 mm W.D.
- Objectives match the refractive index of clearing reagent (ne: 1.41 to 1.52).

3D image of a Sca/eS–treated hemisphere of a 14–week–old YFP–H mouse

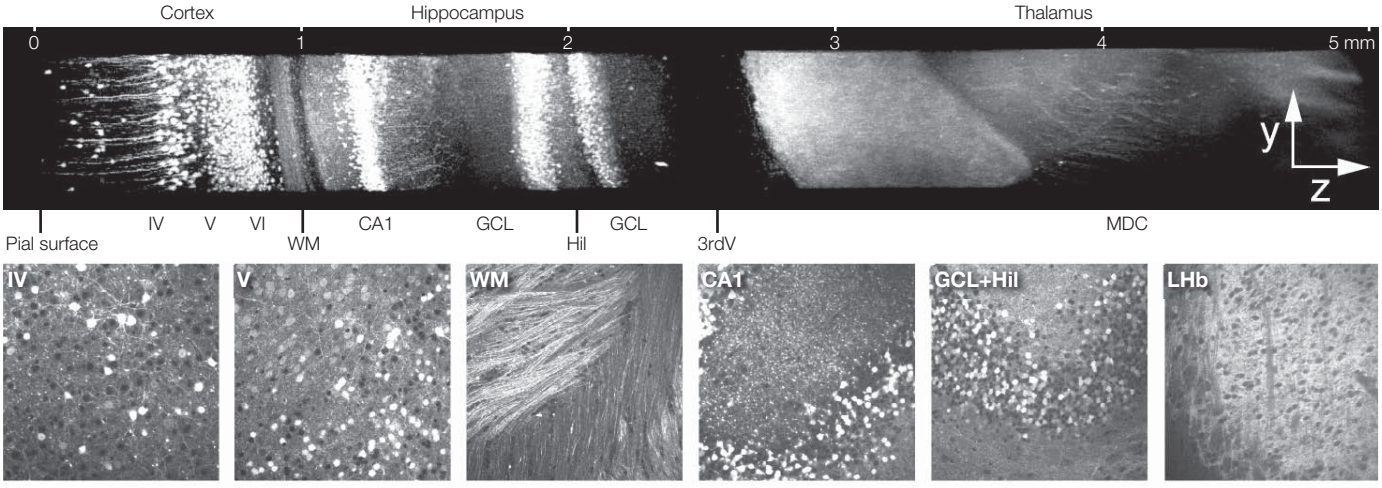

A maximum intensity projection image (top). Six XY images at different Z positions (bottom). WM: white matter; GCL: granule cell layer, Hil: hilus, LHb: lateral habenular nucleus, MDC: mediodorsal thalamic nucleus; scale bars represent 0.1 mm.

Image data courtesy of Hiroshi Hama, Atsushi Miyawaki, RIKEN Brain Science Institute Laboratory for Cell Function Dynamics
Reference: *Nat Neurosci.* 2015 Oct; 18 (10): 1518–29. doi: 10.1038/nn.4107. Epub 2015 Sep 14.

Silicone Immersion Objectives

Distortion–free imaging in live cells and tissues – brighter images, accurate 3D morphology

Silicone immersion objectives are optimized for live cell and live tissue imaging. By properly matching the refractive index, images are clearer and brighter, and time–lapse observations become more reliable and less complex because silicone oil does not dry at 37 °C. Unlike glycerol/water mixtures, the refractive index of silicone oil remains constant, and the resolution is higher than comparable water objectives, helping ensure the accuracy of critical cell and tissue morphology studies. Because the refractive index of silicone immersion oil (ne=1.40) is close to that of the clearing reagent SCALEVIEW–A2 (ne=1.38), the silicone immersion objectives are also well suited for observing SCALEVIEW–A2 cleared samples.

Selection Guide for Silicone Immersion Objectives

	W.D. (mm)	MAG.	FN*	NA	Immersion	Applications
UPLSAPO100XS	0.2	100X	22	1.35	Silicone oil	High–resolution for subcellular imaging
UPLSAPO60XS2	0.3	60X	22	1.30	Silicone oil	High–resolution and long–term time–lapse imaging of single cells
UPLSAPO40XS	0.3	40X	22	1.25	Silicone oil	Multiple cell imaging with submicron resolution
UPLSAPO30XS	0.8	30X	22	1.05	Silicone oil	Deeper tissue imaging with a wider field of view
UPLSAPO30XSIR	0.8	30X	22	1.05	Silicone oil	MPE imaging in deep tissue with a wider field of view

*Maximum field number observable through eyepiece.

Effects of Refractive Index Mismatch on Sample Shape

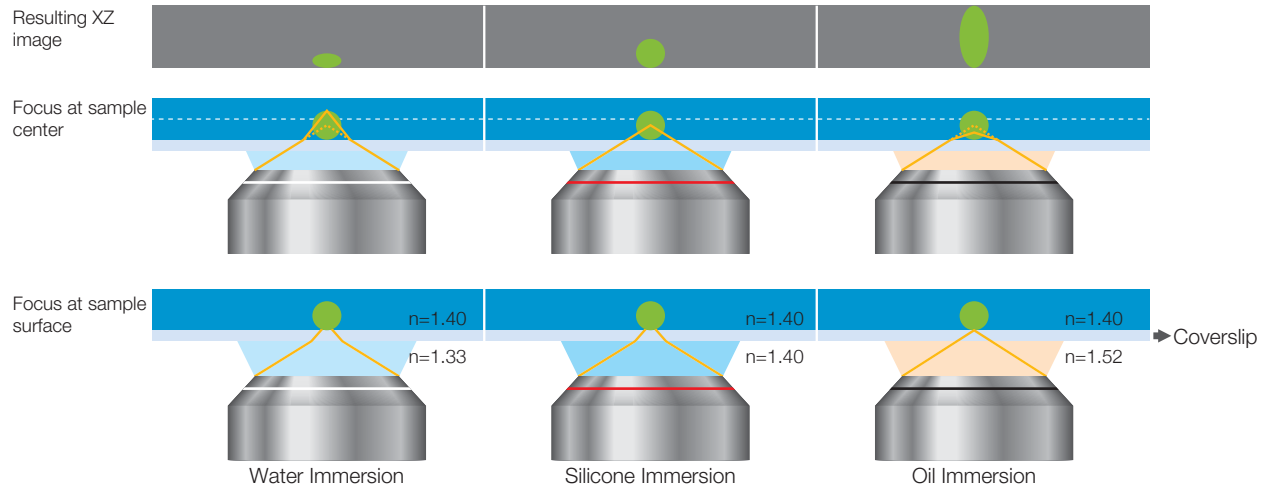

Matching the refractive index of a sample and immersion media is very important to get accurate 3D images.

Brightness Comparison of 60X Objectives

Normalized by the brightness of 60X objective at sample surface sample refractive index: 1.38.

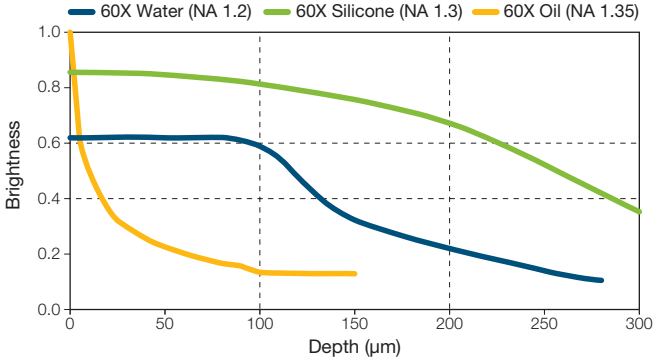

Oil immersion objectives are brightest at superficial depths. Silicone immersion objectives are brighter than water immersion objectives at all focus depths for a given magnification.

Comparison of Silicone and Oil Immersion 60X Objectives

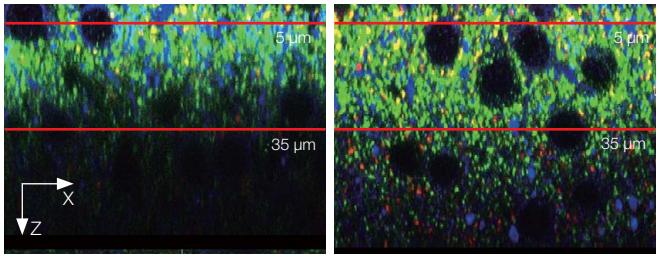

UPLSAPO 60XO
(NA 1.3, W.D. 0.3 mm, immersion oil ne = 1.52)

UPLSAPO60XS2
(NA 1.3, W.D. 0.3 mm, silicone oil ne = 1.4)

By matching the refractive index of the sample and immersion medium, the silicone objective (UPLSAPO60XS2) enables deeper imaging.
Sample: Sca/eA2–treated neocortex, VGluT1/Green, VGluT2/Red, MAP2/Blue

Image data courtesy of Motokazu Uchigashima, M.D., Ph.D., Masahiko Watanabe, M.D., Ph.D., Departments of Anatomy, Hokkaido University Graduate School of Medicine

Long–Term Time–Lapse Imaging of a Live Mouse Embryo (UPLSAPO60XS2)

- High–resolution imaging with 1.30 NA, 3D imaging with 0.3 mm W.D.
- Long–term time–lapse imaging with stable silicone immersion oil.

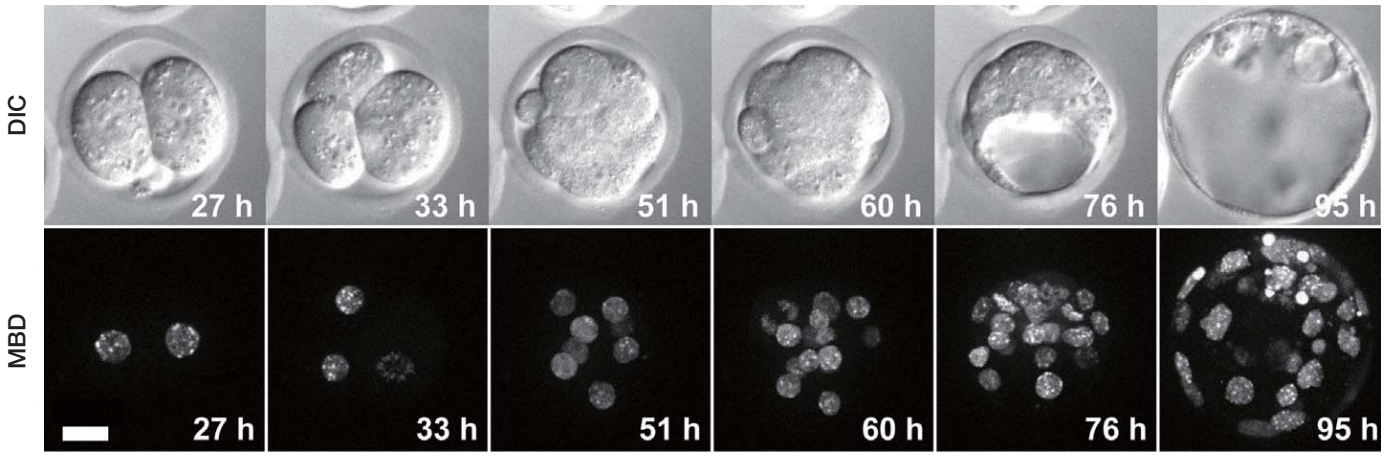

Long–term time–lapse images of a live mouse embryo. Images were taken every hour from the zygote (0 h) to blastocyst (119 h) stage. mCherry–fused methyl–CpG–binding domain (MBD) of MBD1 protein. Images acquired using silicone immersion objecive UPLSAPO60XS. Scale bar, 20 µm.

Image data courtesy of Kazuo Yamagata Ph.D., Faculty of Biology–Oriented Science and Technology, Kinki University
Reference Stem: *Cell Reports.* 2014 Jun 3; 2 (6): 910–924.

Deep Observation of a Whole Placenta Rendered Transparent by Sca/eU2 Clearing Reagent (UPLSAPO40XS)

- Matches the refractive index of the clearing reagent Sca/eU2 for higher resolution and brighter images.
- Minimizes chromatic aberration to deliver accurate co–localization.
- Deep imaging area with 0.3 mm W.D. and NA 1.25.

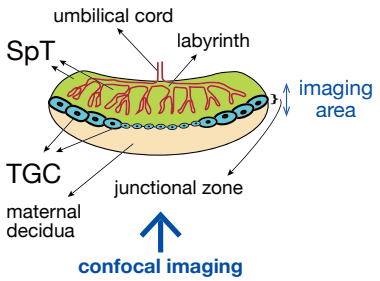

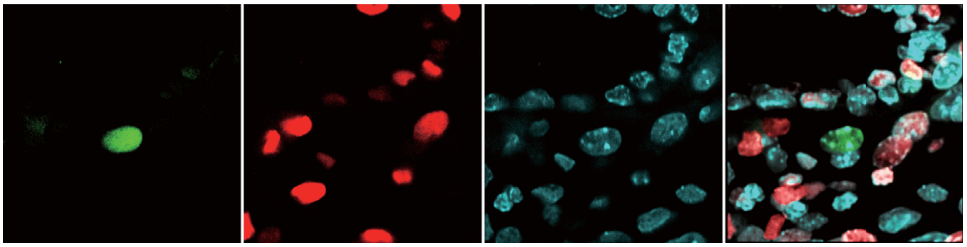

Observation of cells within a whole mouse placenta (E10.5)—sequential tomography.
The whole placenta (E10.5) of a transgenic mouse that expresses fluorescent ubiquitination–based cell cycle indicator (Fucci) was treated with a clearing reagent (Sca/eU2) that renders biological tissue transparent.
Fucci (S/G2/M–Green, G1–Red) and the nuclei (DAPI staining–Blue).

Image data courtesy of Asako Sakaue–Sawano, Atsushi Miyawaki, RIKEN Brain Science Institute Laboratory for Cell Function Dynamics
Reference: *Development.* 2013 Nov; 140 (22): 4624–32. doi: 10.1242/dev.099226. Epub 2013 Oct 23.

Long–Term Live–Cell Imaging of *Arabidopsis* Zygote Embryogenesis (UPLSAPO30XS)

- Higher resolution and brighter images with NA 1.05.
- Wider field of view and deeper imaging with 0.8 mm W.D.

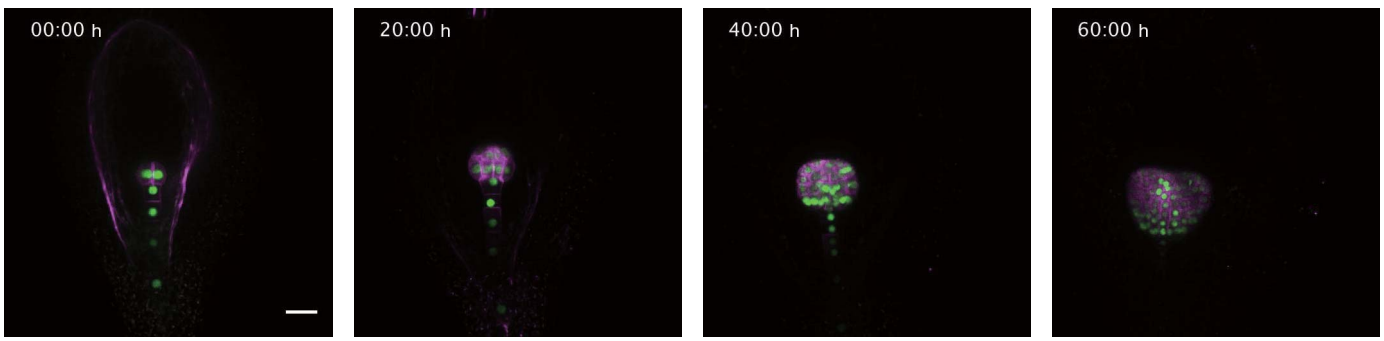

The process of embryogenesis from the early embryo (4–cell stage) to the late embryo was recorded over 60 hours. Nucleus and plasma membrane are labeled green (H2B–GFP) and magenta (tdTomato–LTI6b). Scale bars represent 30 µm.

Image data courtesy of Daisuke Kurihara, Ph.D., Optical Technology Group, ERATO Higashiyama Live–Holonics Project, Nagoya University
Reference: *Dev Cell.* 2015 Jul 27; 34 (2): 242–51. doi: 10.1016/j.devcel.2015.06.008. Epub 2015 Jul 9.

TIRF (Total Internal Reflected Fluorescence) Objectives

Olympus is a pioneer in the field of TIRF microscopy, and our range of TIRF objectives is designed to provide tight control over the evanescent waves produced in TIRF with magnifications from 60X–150X and high NAs of 1.45, 1.49, and the world's highest 1.7*1. Such high NAs not only provide high resolution but make it easier to adjust the critical angle and evanescent wave penetration depth. Each objective has a correction collar enabling optimization for coverslip thickness. Whether conducting traditional TIRF experiments or extending to Olympus Super Resolution – OSR – these high NA objectives can be an essential part of an experiment.

*1 As of May 31, 2016. According to Olympus research.

Selection Guide of TIRF Objectives

	W.D. (mm)	MAG.	FN*2	NA	Immersion	Applications
APON60XOTIRF	0.1	60X	22	1.49	Oil	Whole cell TIRF imaging
UAPON100XOTIRF	0.1	100X	22	1.49	Oil	High–resolution imaging of cell membranes or subcellular organelle and single molecule level experiments
APON100XHOTIRF	0.08	100X	22	1.70	Special Oil	Observing movement of proteins or vesicles at the single molecule level
UAPON150XOTIRF	0.08	150X	22	1.45	Oil	Subcellular imaging (e.g. organelle, endoplasmic reticulum, and intracellular vesicle trafficking)

*2 Maximum field number observable through eyepiece.

Time–Lapse TIRF Imaging of Polymerization and Depolymerization Between Plasma Membrane and FBP17 Membrane–Bending Protein (UAPON100XOTIRF)

- Adjusted penetration depth to get a high signal–to–noise ratio with NA 1.49.

A Schematic Overview of Feedback Loop Between Plasma Membrane Tension and FBP17

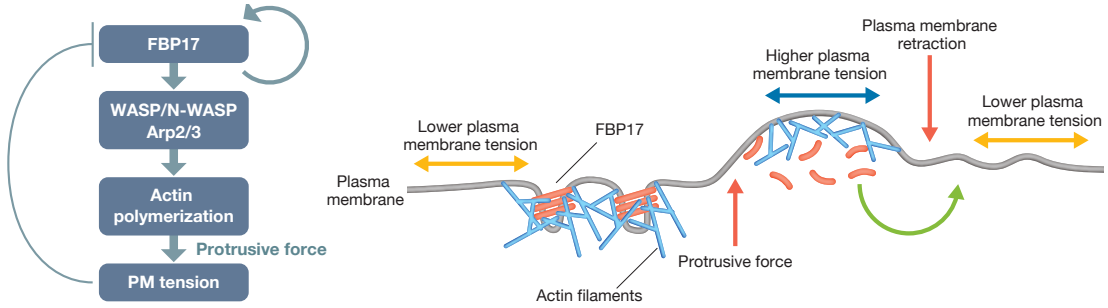

Time–Lapse Images of Cos–1 Cell Co–Expressing GFP–FBP17 and Lifeact–mCherry

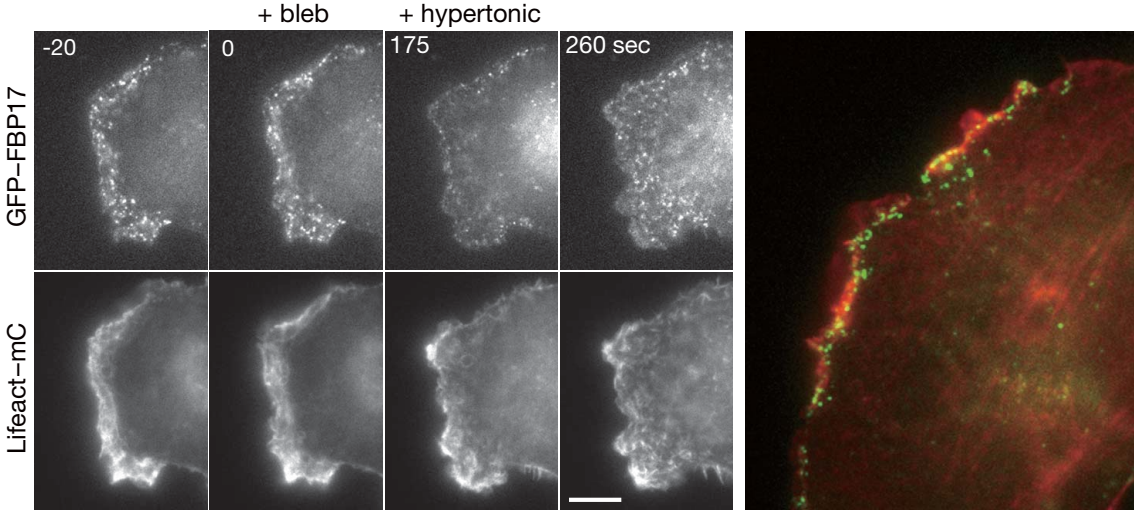

Examining whether the recruitment of FBP17 to the plasma membrane is dependent on transient reduction of membrane tension caused by myosin–based contraction force. FBP17 acutely disappeared from the cell edge after treatment with the myosin inhibitor blebbistatin (175 sec). Scale bar, 10 µm.

Image data courtesy of Kazuya Tsujita, Ph.D., Toshiki Itoh, Ph.D., Biosignal Research Center, Organization of Advanced Science and Technology, Kobe University
Reference: *Nat Cell Biol.* 2015 Jun; 17 (6): 749–58. doi: 10.1038/ncb3162.

Single–Molecule Fluorescence Imaging to Count the Subunits of a Transmembrane Ion Channel Complex (APON100XHOTIRF)

• Single molecule TIRF imaging with higher resolution and brighter images with NA 1.70.

The subunit counting technique was used to analyze the number of accessory dipeptidyl peptidase–like protein 10 (DPP10) molecules, which bind to the transmembrane ion channel Kv4.2, in one Kv4.2–DPP10 complex.
The subunit counting*1 used in this study required continuous fluorescence photobleaching of proteins (subunits) that are tagged with a fluorescent protein –such as a monomeric enhanced green fluorescent protein (mEGFP)– by excitation laser for around 10 seconds and live monitoring of the photobleaching process using single–molecule fluorescence imaging. At the single molecule level, fluorescence photobleaching is stepwise based on the number of fluorescent molecules. Therefore, the number of DPP10 molecules can be determined by counting the stepwise photobleaching events at the spots where Kv4.2–mCherry and mEGFP–DPP10 colocalize. The world's highest NA*2 of the APON100XHOTIRF objective enables researchers to measure fluorescence intensity change caused by photo–bleaching of single molecule. This study*3 revealed that a maximum of 4 molecules of DPP10 subunits form a complex with the ion channel Kv4.2.

*1 Ulbrich, MH, and Isacoff EY. "Subunit counting in membrane–bound proteins." *Nature Methods,* 4 (2007): 319–321.
*2 As of May 31, 2016. According to Olympus research.
*3 Kitazawa M, Kubo Y, and Nakajo K. "Kv4.2 and accessory dipeptidyl peptidase–like protein 10 (DPP10) subunit preferentially form a 4:2 (Kv4.2:DPP10) channel complex." *J Biol Chem,* 290 (2015): 22724–22733.

Schematic Illustration of Subunit Counting of a Transmembrane Ion Channel Complex Using Single–Molecule Fluorescence Imaging

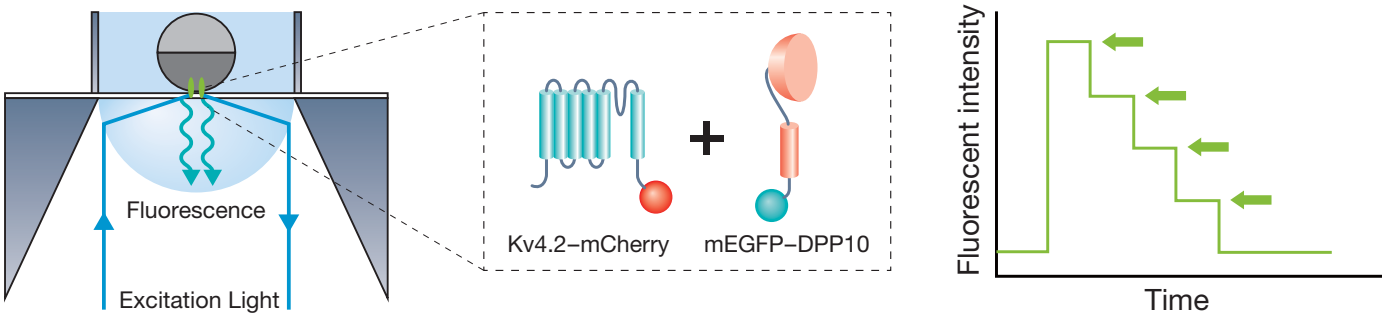

- Counting of step–wise bleaching events at a spot where two colors colocalize.
- The number of steps is equal to the number of molecules in the complex.

Determining the Subunit Stoichiometry of the Kv4.2–DPP10 Channel Complex by Subunit Counting

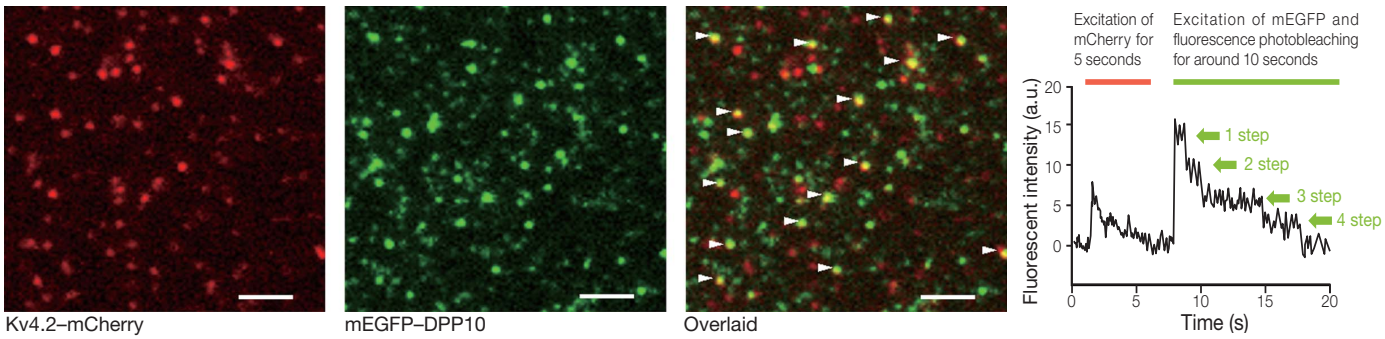

Localization of Kv4.2–mCherry is visualized by excitation of mCherry in the first 5 seconds, followed by excitation of mEGFP in the next 10 seconds to visualize its localization and continuous fluorescence photobleaching. Spots with photobleaching of mEGFP in a maximum of 4 steps were found by graphing the change in fluorescence intensity at each spot where two colors of fluorescent molecules colocalized (indicated by the white arrow head). Therefore, it was found that a maximum of 4 molecules of mEGFP–DPP10 were bound in the Kv4.2 ion channel complexes. Scale bar, 20 µm.

Image data courtesy of; Masahiro Kitazawa, Ph.D., Yoshihiro Kubo, M.D.,Ph.D., Koichi Nakajo*, Ph.D. , Division of Biophysics and Neurobiology, Department of Molecular Physiology, National Institute for Physiological Sciences
*Present address: Department of Physiology, Osaka Medical College

Super–Corrected 60X Objective

Are your fluorescence signals really colocalized? Answering this question with standard fluorescence microscopy requires a superior optical design that corrects for color shifts (aberration) that occur when light passes through an objective. Doing this with just 2 or 3 colors is becoming increasingly insufficient. The super–corrected 60X OSC objective corrects for a broad range of color aberration to provide images that capture fluorescence in the proper location. Save time and resources with multicolor labeling experiments without having to go through post–processing adjustments.

PLAPON60XOSC2

W.D. (mm)	0.12
MAG.	60X
FN*	22
NA	1.40
Immersion	Oil

*Maximum field number observable through eyepiece.

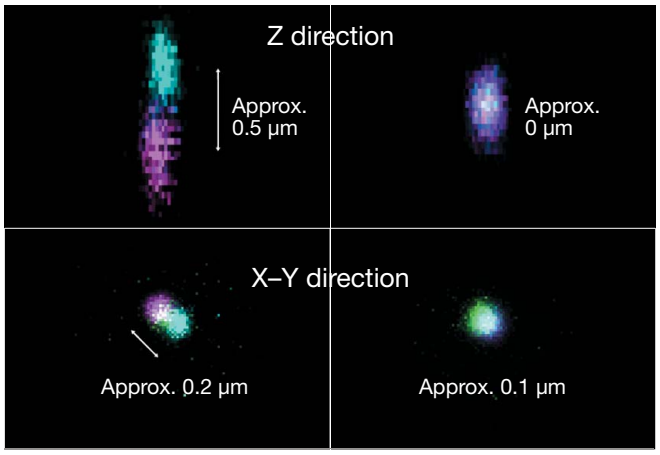

UPLSAPO 60XO PLAPON60XOSC2

Axial chromatic aberration compared for PSF fluorescent beads (405 nm, 633 nm).

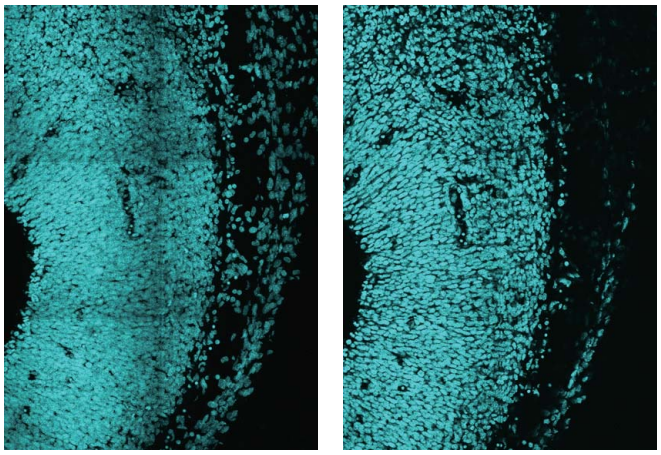

UPLSAPO 60XO PLAPON60XOSC2

Due to the excellent performance of maintaining image flatness, the PLAPON60XOSC2 objective has better stitching capabilities than apochromat objectives (UPLSAPO60XO).

The high NA PLAPON60XOSC2 oil–immersion objective minimizes chromatic aberration in the 405–650 nm region for enhanced imaging performance and image resolution at 405 nm. The objective delivers a high degree of correction for both lateral and axial chromatic aberration to acquire 2D and 3D images with excellent reliability, accuracy, and improved colocalization analysis. The objective also compensates for chromatic aberration in the near infrared up to 850 nm.

Quadruple Immunofluorescence of Brain Tissue

- Improved detection sensitivity and resolution.
- Minimizes chromatic aberrations, ideal for immunofluorescence applications.

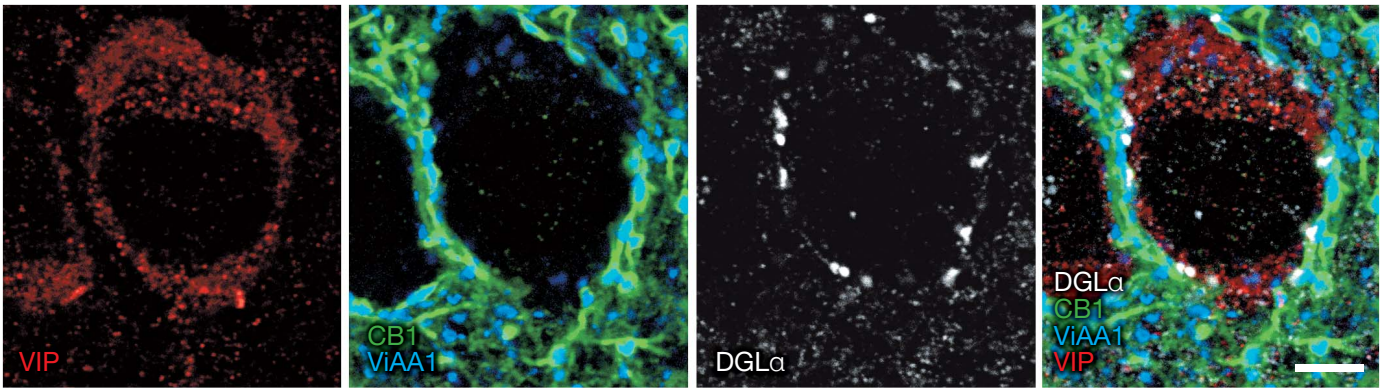

Quadruple immunofluorescence for multiple functional molecules and cell markers can provide detailed information on cell expression and subcellular localization, which includes the codependent or independent relationship between related functional cells and intercellular spatial distances. ViAA1 (Alexa Fluor405, blue), CB1 (Alexa Fluor488, green), VIP (Cy3, red), and DGLα (Alexa Fluor647, white). Scale bar, 5 µm.

Image data courtesy of Masahiko Watanabe, M.D., Ph.D. ,Departments of Anatomy, Hokkaido University Graduate School of Medicine
Reference: *J Neurosci.* 2015 Mar 11; 35 (10): 4215–28. doi: 10.1523/JNEUROSCI.4681–14.2015.

A Time Saving Objective for Plastic Bottom Plates and Dishes

Your experiment time is valuable, and every extra step required in the process takes time away from your research goals. Inspecting tissue culture with phase contrast and fluorescence imaging and having confidence in fluorescent protein expression levels has often meant first culturing tissue in plastic bottom dishes for adherence and then transferring the culture to glass chambers for imaging. With the UCPLFLN20XPH objective, you can skip the step of re–plating cells in glass chambers. Designed for both fluorescence and phase imaging of tissue in plastic bottom dishes, the UCPLFLN20XPH objective improves workflow. With its high NA, images are bright and even across the objective's large field of view and the correction collar and long working distance optimizes images through different cell culture vessels.

UCPLFLN20XPH

W.D. (mm)	0.8 – 1.2
MAG.	20X
FN*	22
NA	0.70
Immersion	Dry

*Maximum field number observable through eyepiece.

Improve the Workflow of Culturing Cells

- Simplifying the workflow for fluorescence observation.
- No longer necessary to subculture, which often requires an extra coating step.

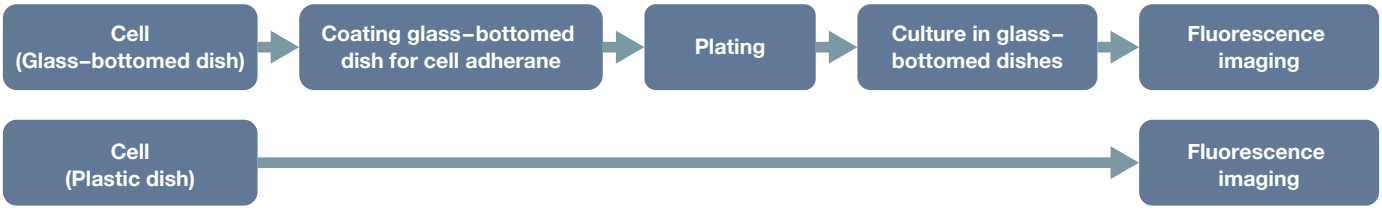

ES Cells expressing GFP–H2B in 35 mm plastic bottom cell culture dish

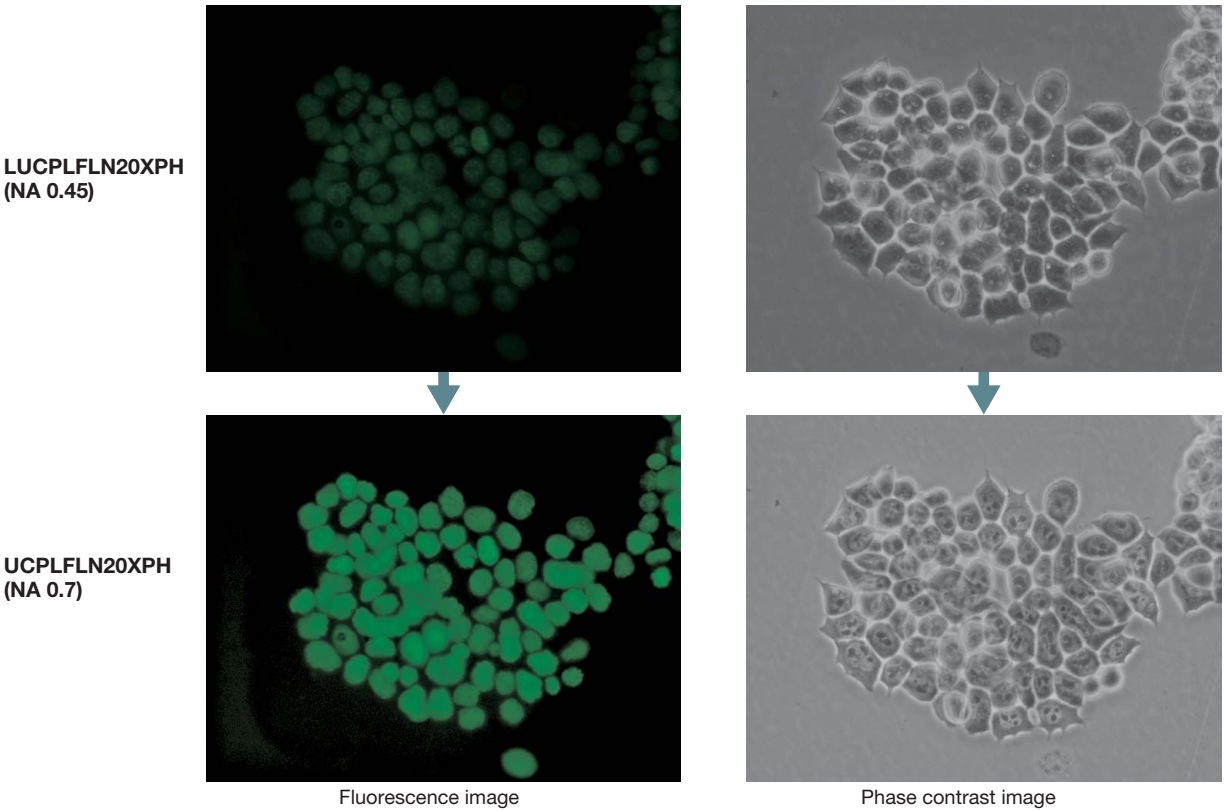

Bright fluorescence observation of histones in the nuclei (GFP–H2B) and phase contrast observation of nucleolus are possible with a high degree of detail.

Image data courtesy of: Tomonobu Watanabe, Ph.D., Laboratory for Comprehensive Bioimaging, RIKEN Quantitative Biology Center

Olympus Immersion Oils

Low Autofluorescence Immersion Oil

IMMOIL–F30CC

- 1/10 the level of autofluorescence compared to standard oil
- Low odor – MSDS available

Silicone Immersion Oil

SIL300CS–30SC

- Refractive index: ne=1.406 at 23 ℃
- Net 30 mL
- Low autofluorescence

List of Reference Articles Using Olympus High End Objectives

MPE Dedicated Objectives

Neuron Published online 24 March 2016

Cooperative Subnetworks of Molecularly Similar Interneurons in Mouse Neocortex
Mahesh M. Karnani, Jesse Jackson, Inbal Ayzenshtat, Jason Tucciarone, Kasra Manoocheri, William G. Snider, Rafael Yuste

Science Published online 24 March 2016

Nuclear envelope rupture and repair during cancer cell migration
CELINE M. DENAIS, RACHEL M. GILBERT, PHILIPP ISERMANN, ALEXANDRA L. MCGREGOR, MARISKA TE LINDERT, BETTINA WEIGELIN, PATRICIA M. DAVIDSON, PETER FRIEDL, KATARINA WOLF, JAN LAMMERDING

Nature Communications Published online 22 March 2016

Calcium imaging reveals glial involvement in transcranial direct current stimulation–induced plasticity in mouse brain
Hiromu Monai, Masamichi Ohkura, Mika Tanaka, Yuki Oe, Ayumu Konno, Hirokazu Hirai, Katsuhiko Mikoshiba, Shigeyoshi Itohara, Junichi Nakai, Youichi Iwai, Hajime Hirase

Science Published online 4 March 2016

Visualizing antibody affinity maturation in germinal centers
JEROEN M. J. TAS, LUKA MESIN, GIULIA PASQUAL, SASHA TARG, JOHANNE T. JACOBSEN, YASUKO M. MANO, CASIE S. CHEN, JEAN–CLAUDE WEILL, CLAUDE–AGNÈS REYNAUD, EDWARD P. BROWNE, MICHAEL MEYER–HERMANN, GABRIEL D. VICTORA

Neuron Published online 7 January 2016

Simultaneous Multi–plane Imaging of Neural Circuits
Weijian Yang, Jae–eun Kang Miller, Luis Carrillo–Reid, Eftychios Pnevmatikakis, Liam Paninski, Rafael Yuste, Darcy S. Peterka

Nature Neuroscience Published online 21 December 2015

Thalamus provides layer 4 of primary visual cortex with orientation– and direction–tuned inputs
Wenzhi Sun, Zhongchao Tan, Brett D Mensh & Na Ji

Cell Published online 3 December 2015

Simple, Scalable Proteomic Imaging for High–Dimensional Profiling of Intact Systems
Evan Murray, Jae Hun Cho, Daniel Goodwin, Taeyun Ku, Justin Swaney, Sung–Yon Kim, Heejin Choi, Young–Gyun Park, Jeong–Yoon Park, Austin Hubbert, Margaret McCue, Sara Vassallo, Naveed Bakh, Matthew P. Frosch, Van J. Wedeen, H. Sebastian Seung, Kwanghun Chung

Nature Published online 9 September 2015

Labelling and optical erasure of synaptic memory traces in the motor cortex
Akiko Hayashi–Takagi, Sho Yagishita, Mayumi Nakamura, Fukutoshi Shirai, Yi Wu, Amanda L. Loshbaugh, Brian Kuhlman, Klaus M. Hahn, and Haruo Kasai

Silicone Immersion Objectives

Nature Published online 9 March 2016

Tip–localized receptors control pollen tube growth and LURE sensing in Arabidopsis
Hidenori Takeuchi & Tetsuya Higashiyama

Acta Neuropathologica Published online 7 March 2016

ECEL1 mutation implicates impaired axonal arborization of motor nerves in the pathogenesis of distal arthrogryposis
Kenichi Nagata, Sumiko Kiryu–Seo, Hiromi Tamada, Fumi Okuyama–Uchimura, Hiroshi Kiyama, Takaomi C. Saido

Development Published online 18 February 2016

The ciliary marginal zone of the zebrafish retina: clonal and time–lapse analysis of a continuously growing tissue
Yinan Wan, Alexandra D. Almeida, Steffen Rulands, Naima Chalour, Leila Muresan, Yunmin Wu, Benjamin D. Simons, Jie He, William A. Harris

TIRF (Total Internal Reflection Fluorescence) Objectives

Nature Biotechnology Published online 18 April 2016

Multiplexed labeling of genomic loci with dCas9 and engineered sgRNAs using CRISPRainbow
Hanhui Ma, Li–Chun Tu, Ardalan Naseri, Maximiliaan Huisman, Shaojie Zhang, David Grunwald & Thoru Pederson

The Journal of Cell Biology Published online 11 April 2016

Sigma1 receptors inhibit store–operated Ca2+ entry by attenuating coupling of STIM1 to Orai1
Shyam Srivats, Dilshan Balasuriya, Mathias Pasche, Gerard Vistal, J. Michael Edwardson, Colin W. Taylor, and Ruth D. Murrell–Lagnado

Nature Chemical Biology Published online 4 April 2016

Raft–based interactions of gangliosides with a GPI–anchored receptor
Naoko Komura, Kenichi G N Suzuki, Hiromune Ando, Miku Konishi, Machi Koikeda, Akihiro Imamura, Rahul Chadda, Takahiro K Fujiwara, Hisae Tsuboi, Ren Sheng, Wonhwa Cho, Koichi Furukawa, Keiko Furukawa, Yoshio Yamauchi, Hideharu Ishida, Akihiro Kusumi & Makoto Kiso

Nature Immunology Published online 21 March 2016

Initiation of T cell signaling by CD45 segregation at 'close contacts'
Veronica T Chang, Ricardo A Fernandes, Kristina A Ganzinger, Steven F Lee, Christian Siebold, James McColl, Peter Jönsson, Matthieu Palayret, Karl Harlos, Charlotte H Coles, E Yvonne Jones, Yuan Lui, Elizabeth Huang, Robert J C Gilbert, David Klenerman, A Radu Aricescu & Simon J Davis

Nature Chemical Biology Published online 29 February 2016

Direct observation of intermediate states during the stepping motion of kinesin–1
Hiroshi Isojima, Ryota Iino, Yamato Niitani, Hiroyuki Noji & Michio Tomishige

Cell Published online 14 January 2016

Integrins Form an Expanding Diffusional Barrier that Coordinates Phagocytosis
Spencer A. Freeman, Jesse Goyette, Wendy Furuya, Elliot C. Woods, Carolyn R. Bertozzi, Wolfgang Bergmeier, Boris Hinz, P. Anton van der Merwe, Raibatak Das, Sergio Grinstein

Cell Published online 19 November 2015

Hippocampal Dopamine/DRD1 Signaling Dependent on the Ghrelin Receptor
Andras Kern, Maria Mavrikaki, Celine Ullrich, Rosie Albarran–Zeckler, Alicia Faruzzi Brantley, Roy G. Smith

Super–Corrected 60X Objective

PNAS Published online 25 March 2016

Dopamine synapse is a neuroligin–2–mediated contact between dopaminergic presynaptic and GABAergic postsynaptic structures
Motokazu Uchigashima, Toshihisa Ohtsuka, Kazuto Kobayashi, and Masahiko Watanabe

The Journal of Cell Biology Published online 19 October 2015

Nup132 modulates meiotic spindle attachment in fission yeast by regulating kinetochore assembly
Hui–Ju Yang, Haruhiko Asakawa, Tokuko Haraguchi, and Yasushi Hiraoka

- **OLYMPUS CORPORATION is ISO14001 certified.**
- **OLYMPUS CORPORATION is ISO9001 certified.**

www.olympus-lifescience.com

OLYMPUS®

For enquiries - contact
www.olympus-lifescience.com/contact-us

OLYMPUS CORPORATION
Shinjuku Monolith, 2-3-1 Nishi-Shinjuku, Shinjuku-ku, Tokyo 163-0914, Japan

OLYMPUS EUROPA SE & CO. KG
Wendenstrasse 14-18, 20097 Hamburg, Germany

OLYMPUS CORPORATION OF THE AMERICAS
3500 Corporate Parkway, P.O. Box 610, Center Valley, PA 18034-0610, U.S.A.

OLYMPUS SINGAPORE PTE LTD.
491B River Valley Road, #12-01/04 Valley Point Office Tower, Singapore 248373

OLYMPUS MEDICAL SYSTEMS INDIA PRIVATE LIMITED.
Ground Floor, Tower-C, SAS Tower, The Medicity Complex, Sector-38, Gurgaon 122001, Haryana, India

OLYMPUS LATIN AMERICA, INC.
5301 Blue Lagoon Drive, Suite 290 Miami, FL 33126, U.S.A.

OLYMPUS (CHINA) CO., LTD.
A8F, Ping An International Financial Center, No. 1-3, Xinyuan South Road, Chaoyang District, Beijing, 100027 P.R.C.

OLYMPUS KOREA CO., LTD.
8F Olympus Tower, 446 Bongeunsa-ro, Gangnam-gu, Seoul, 06153 Korea

OLYMPUS AUSTRALIA PTY. LTD.
3 Acacia Place, Notting Hill VIC 3168, Australia

N8600506-082016